Can one study timelike Compton scattering at LHC and at JLab?

Lech Szymanowski

SINS, Warsaw/CPhT, Palaiseau/LPT, Orsay

in collaboration with
B. Pire (CPhT, Palaiseau) and J. Wagner (SINS, Warsaw)

Phys.Rev.D79:014010 (2009), Phys.Rev.D83:034009 (2011)

Spa, 6-8/04/2011

Kinematics of TCS

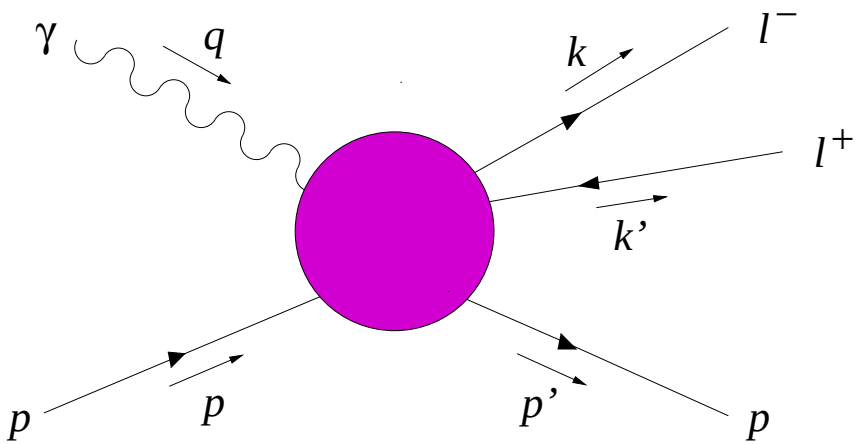

Figure: Real photon-proton scattering into a lepton pair and a proton.

$$\gamma(q)N(p) \to \gamma^*(q')N(p') \to l^-(k)l^+(k')N(p')$$

at small $t = (p' - p)^2$ and large *timelike* virtuality $(k + k')^2 = q'^2 = Q'^2$ of the final state dilepton, timelike Compton scattering (TCS), shares many features with DVCS.

Experiments: JLab (low energy), RHIC and LHC (ultraperipheral)

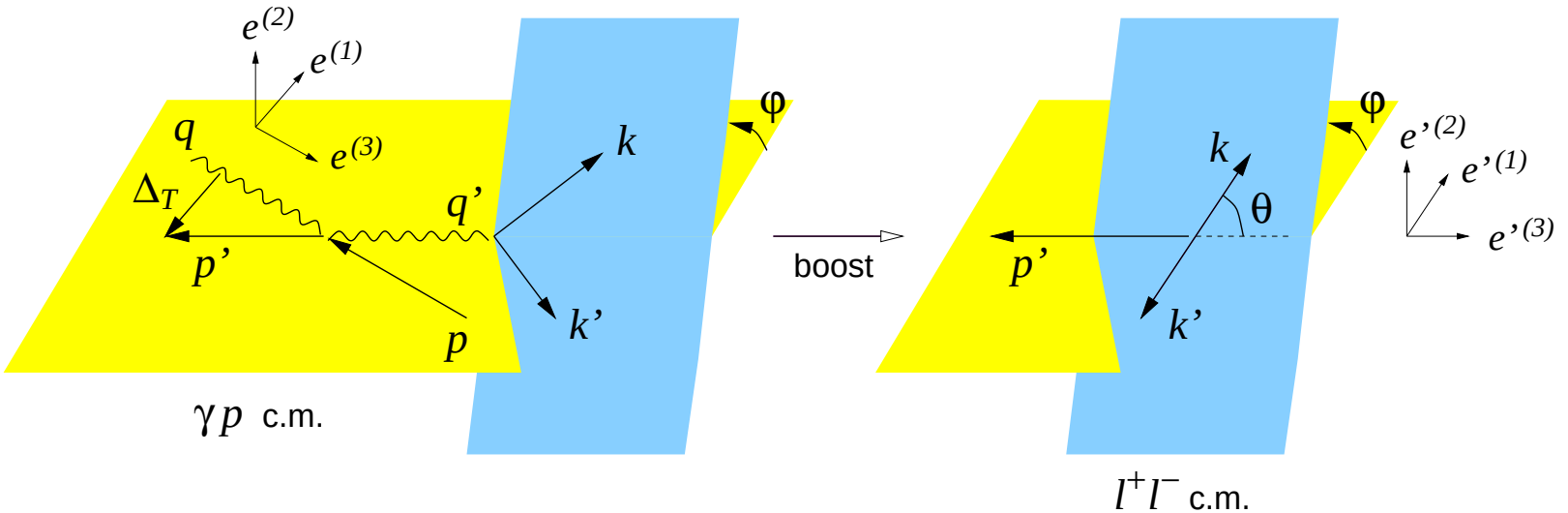

Figure: Kinematical variables and coordinate axes in the γp and $\ell^+\ell^-$ c.m. frames.

The Bethe-Heitler contribution

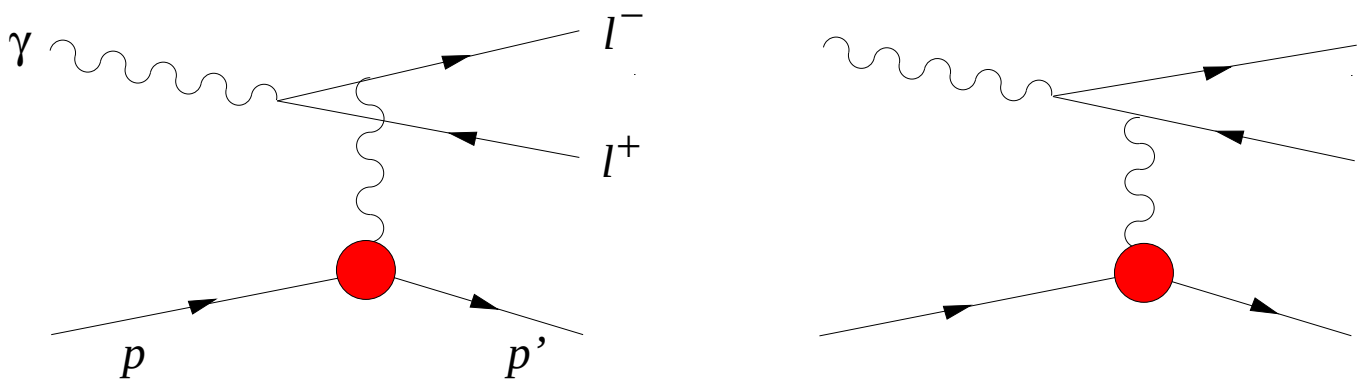

Figure: The Feynman diagrams for the Bethe-Heitler amplitude.

$$\frac{d\sigma_{BH}}{dQ'^2\,dt\,d(\cos\theta)\,d\varphi} \approx \frac{\alpha_{em}^3}{2\pi s^2}\,\frac{1}{-t}\,\frac{1+\cos^2\theta}{\sin^2\theta}\left[\left(F_1^2 - \frac{t}{4M^2}F_2^2\right)\frac{2}{\tau^2}\,\frac{\Delta_T^2}{-t} + (F_1+F_2)^2\right]$$

For small θ BH contribution becomes very large

The Compton contribution

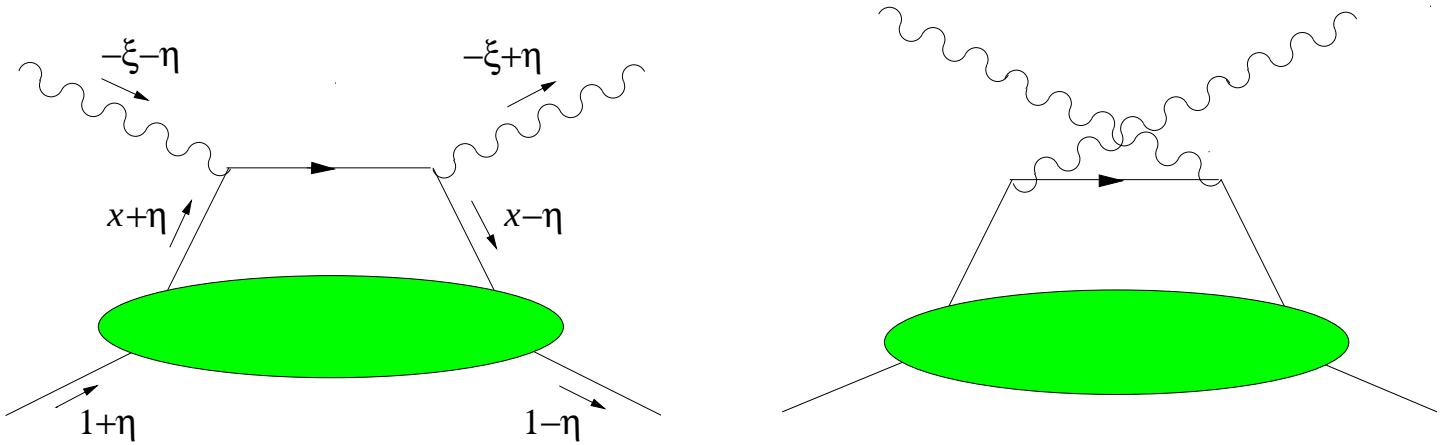

Figure: Handbag diagrams for the Compton process in the scaling limit. The plus-momentum fractions x, ξ, η refer to the average proton momentum $\frac{1}{2}(p+p')$.

$$x = \frac{(k+k')^+}{(p+p')^+},\ \xi \approx -\frac{(q+q')^+}{(p+p')^+},\ \eta \approx \frac{(p-p')^+}{(p+p')^+}.$$

To leading-twist accuracy one has $\xi = -\eta = -\tau/(2-\tau)$, where $\tau = Q'^2/s$ is Björken variable.

the Compton form factors:

$$\begin{aligned}
\mathcal{H}_1(\xi,\eta,t) &= \sum_q e_q^2 \int_{-1}^{1} dx \Big(\frac{1}{\xi - x - i\epsilon} - \frac{1}{\xi + x - i\epsilon}\Big) H^q(x,\eta,t), \\
\mathcal{E}_1(\xi,\eta,t) &= \sum_q e_q^2 \int_{-1}^{1} dx \Big(\frac{1}{\xi - x - i\epsilon} - \frac{1}{\xi + x - i\epsilon}\Big) E^q(x,\eta,t), \\
\tilde{\mathcal{H}}_1(\xi,\eta,t) &= \sum_q e_q^2 \int_{-1}^{1} dx \Big(\frac{1}{\xi - x - i\epsilon} + \frac{1}{\xi + x - i\epsilon}\Big) \tilde{H}^q(x,\eta,t), \\
\tilde{\mathcal{E}}_1(\xi,\eta,t) &= \sum_q e_q^2 \int_{-1}^{1} dx \Big(\frac{1}{\xi - x - i\epsilon} + \frac{1}{\xi + x - i\epsilon}\Big) .\tilde{E}^q(x,\eta,t)
\end{aligned}$$

For example: $M^{\lambda' \lambda^{\gamma^*}, \lambda \lambda^{\gamma}}$

$$M^{+-,+-}\Big|_{TCS} =$$

$$\sqrt{1-\eta^2}(\mathcal{H}_1(-\eta,\eta,t) + \tilde{\mathcal{H}}_1(-\eta,\eta,t) - \frac{\eta^2}{1-\eta^2}(\mathcal{E}_1(-\eta,\eta,t) + \tilde{\mathcal{E}}_1(-\eta,\eta,t)))$$

Modelizing GPDs

Factorized ansatz for t-dependence:

$$\begin{aligned} H^u(x,\eta,t) &= h^u(x,\eta)\frac{1}{2}F_1^u(t) \\ H^d(x,\eta,t) &= h^d(x,\eta)F_1^d(t) \\ H^s(x,\eta,t) &= h^s(x,\eta)F_D(t) \end{aligned}$$

Double distribution ansatz for h^q without any D-term:

$$\begin{aligned} h^q(x,\eta) &= \int_0^1 dx' \int_{-1+x'}^{1-x'} dy' \\ &\quad \Big[\delta(x-x'-\eta y')q(x') - \delta(x+x'-\eta y')\bar{q}(x')\Big]\pi(x',y') \\ \pi(x',y') &= \frac{3}{4}\frac{(1-x')^2 - y'^2}{(1-x')^3} \end{aligned}$$

For the unpolarized distributions $q(x)$ and $\bar{q}(x)$ we take NLO($\overline{\mathrm{MS}}$) GRVGJR 2008 parametrization.

They have strong dependence of the factorization scale choice for small x:

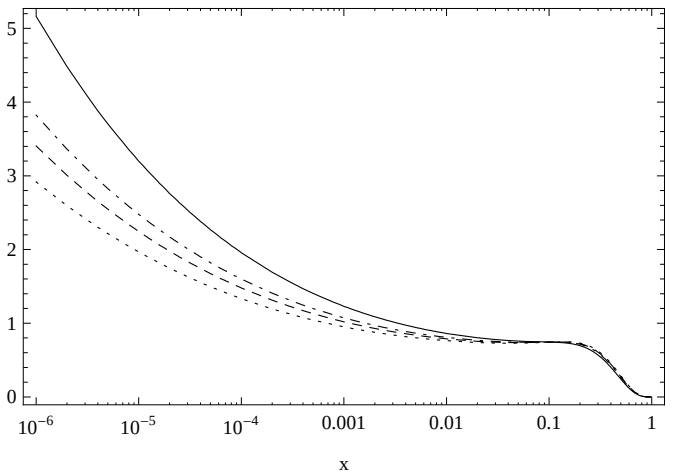

Figure: The NLO($\overline{MS}$) GRVGJR 2008 parametrization of $u(x) + \bar{u}(x)$ for different factorization scales $\mu_F^2 = 4$ (dotted) , 5 (dashed) , 6 (dash-dotted) , 10 (solid) GeV^2.

This results in the strong dependence of h^q for small values of η:

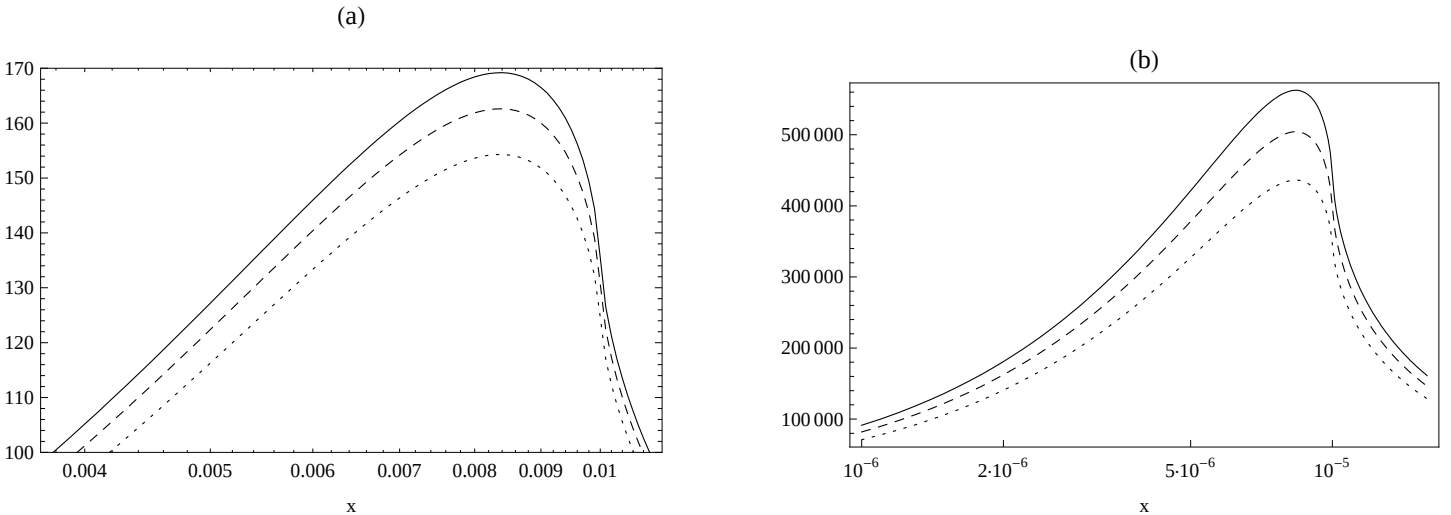

Figure: $h^u_+(x,\eta) = h^u(x,\eta) - h^u(-x,\eta)$ for $\eta = 10^{-2}$ (a) and for $\eta = 10^{-5}$ (b) for different factorization scales $\mu_F^2 = 4$ (dotted) , 5 (dashed) , 6 (solid) GeV^2.

B-H cross section at UPC

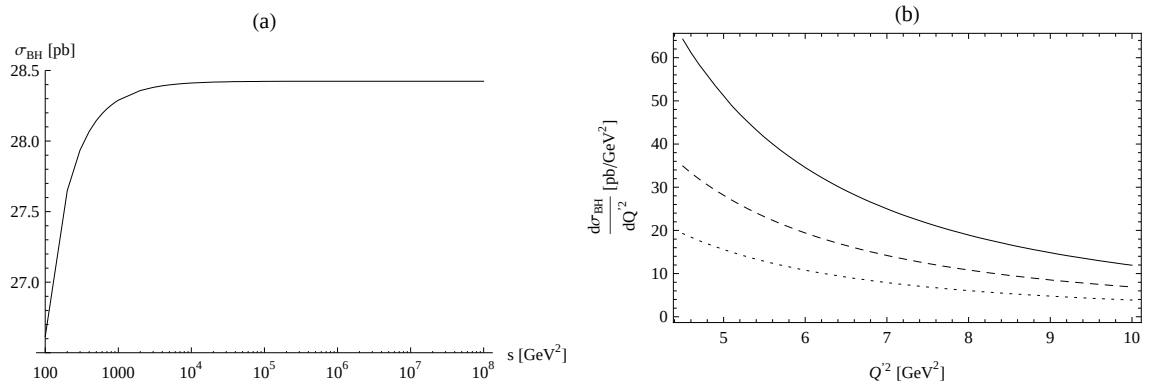

Figure: (a) The BH cross section integrated over $\theta \in [\pi/4, 3\pi/4]$, $\varphi \in [0, 2\pi]$, $Q'^2 \in [4.5, 5.5]\,\mathrm{GeV}^2$, $|t| \in [0.05, 0.25]\,\mathrm{GeV}^2$, as a function of γp c.m. energy squared s. (b) The BH cross section integrated over $\varphi \in [0, 2\pi]$, $|t| \in [0.05, 0.25]\,\mathrm{GeV}^2$, and various ranges of θ : $[\pi/3, 2\pi/3]$ (dotted), $[\pi/4, 3\pi/4]$ (dashed) and $[\pi/6, 5\pi/6]$ (solid), as a function of Q'^2 for $s = 10^5\,\mathrm{GeV}^2$

TCS cross section at UPC

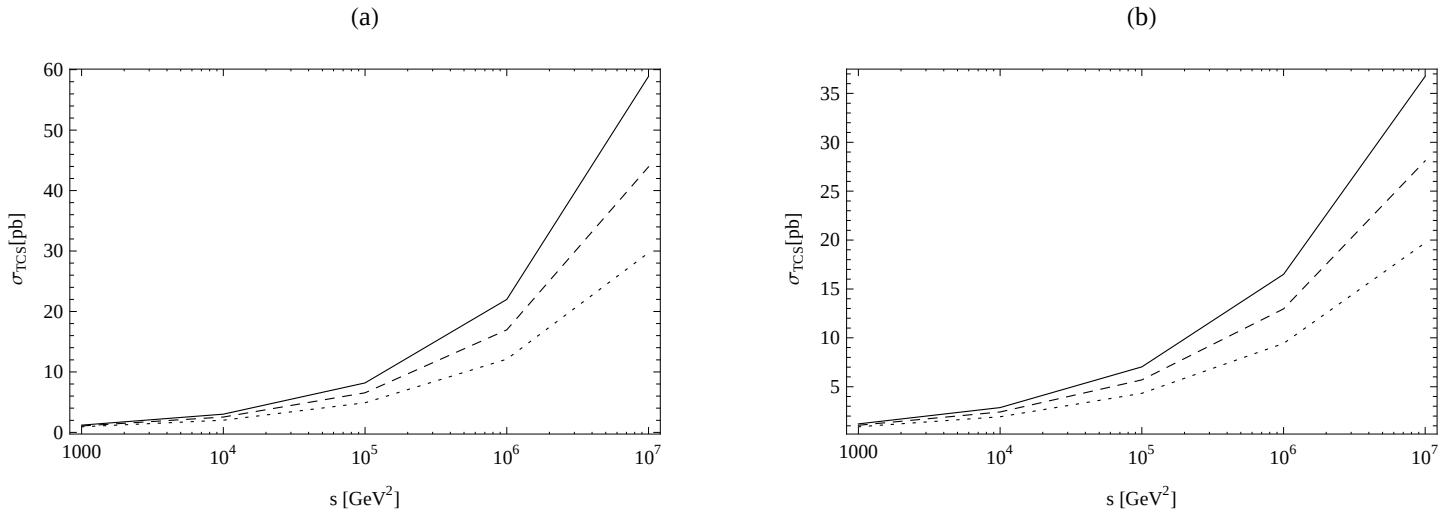

Figure: σ_{TCS} as a function of γp c.m. energy squared s, for GRVGJR2008 LO (a) and NLO (b) parametrizations, for different factorization scales $\mu_F^2 = 4$ (dotted), 5 (dashed), 6 (solid) GeV^2.

For very high energies σ_{TCS} calculated with $\mu_F^2 = 6\,\mathrm{GeV}^2$ is much bigger then with $\mu_F^2 = 4\,\mathrm{GeV}^2$. Also predictions obtained using LO and NLO GRVGJR2008 PDFs differ significantly.

The interference cross section at UPC

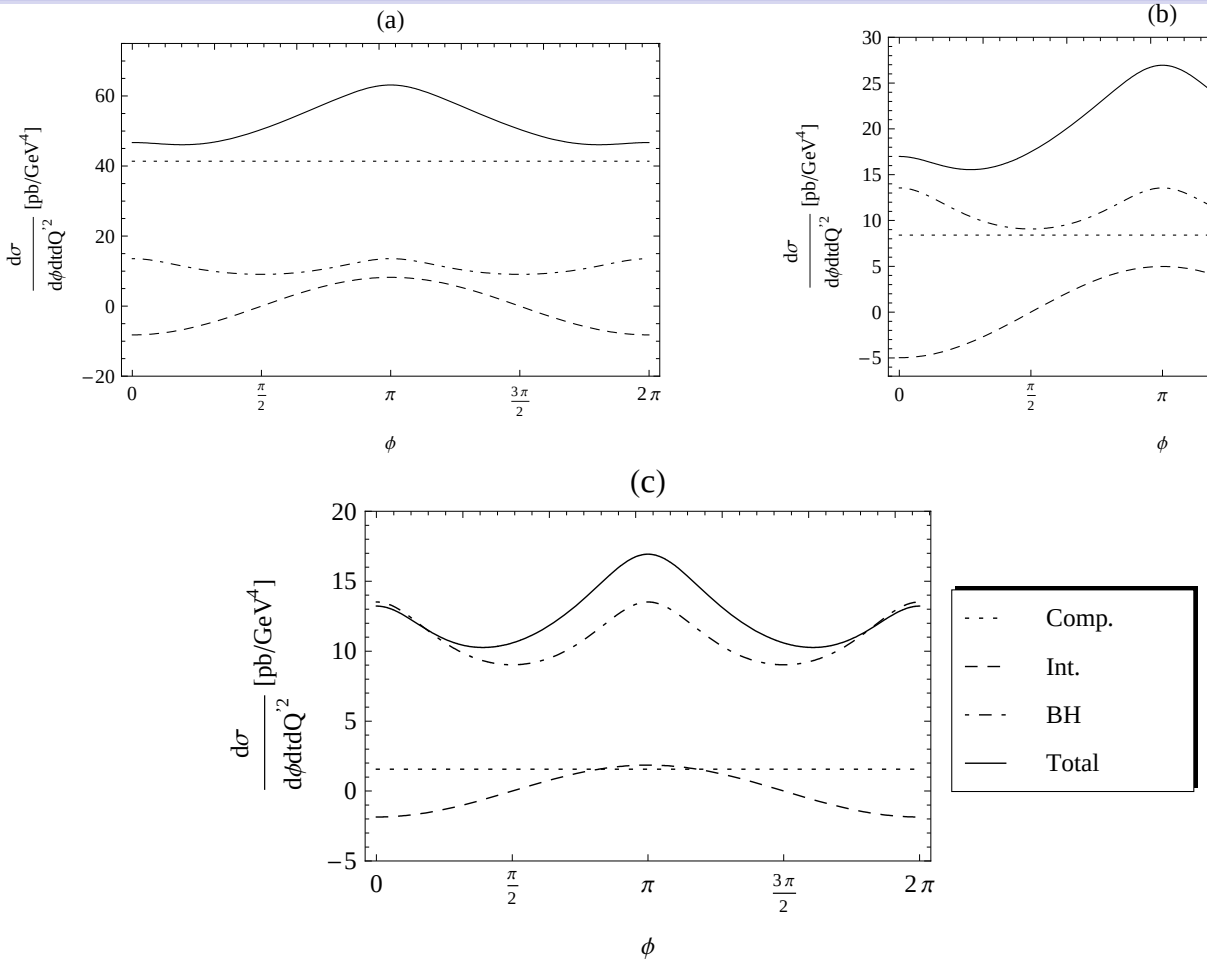

Figure: The differential cross sections (solid lines) for $t = -0.2\,\mathrm{GeV}^2$, $Q'^2 = 5\,\mathrm{GeV}^2$ and integrated over $\theta = [\pi/4, 3\pi/4]$, as a function of φ, for $s = 10^7\,\mathrm{GeV}^2$ (a), $s = 10^5\,\mathrm{GeV}^2$(b), $s = 10^3\,\mathrm{GeV}^2$ (c) with $\mu_F^2 = 5\,\mathrm{GeV}^2$. We also display the Compton (dotted), Bethe-Heitler (dash-dotted) and Interference (dashed) contributions.

Rate estimates for UPC

$$\sigma_{pp} = 2 \int \frac{dn(k)}{dk} \sigma_{\gamma p}(k) dk$$

$\sigma_{\gamma p}(k)$ is the cross section for the $\gamma p \to p l^+ l^-$ process and k is the γ's energy.

$\frac{dn(k)}{dk}$ is an equivalent photon flux

$$\frac{dn(k)}{dk} = \frac{\alpha}{2\pi k}\left[1 + (1 - \frac{2k}{\sqrt{s_{pp}}})^2\right]\left(\ln A - \frac{11}{6} + \frac{3}{A} - \frac{3}{2A^2} + \frac{1}{3A^3}\right)$$

$A = 1 + \frac{0.71\,\mathrm{GeV}^2}{Q^2_{min}}$, $Q^2_{min} \approx \frac{4M_p^2 k^2}{s_{pp}}$ is the minimal $-t$

s_{pp} is the proton-proton energy squared ($\sqrt{s_{pp}} = 14\,\mathrm{TeV}$): $s \approx 2\sqrt{s_{pp}}k$

The pure Bethe - Heitler contribution to σ_{pp}, integrated over $\theta = [\pi/4, 3\pi/4]$, $\phi = [0, 2\pi]$, $t = [-0.05\,\mathrm{GeV}^2, -0.25\,\mathrm{GeV}^2]$, $Q'^2 = [4.5\,\mathrm{GeV}^2, 5.5\,\mathrm{GeV}^2]$, and photon energies $k = [20, 900]\,\mathrm{GeV}$ gives:

$$\sigma_{pp}^{BH} = 2.9\mathrm{pb}\ .$$

The Compton contribution (calculated with NLO GRVGJR2008 PDFs, and $\mu_F^2 = 5\,\mathrm{GeV}^2$) gives:

$$\sigma_{pp}^{TCS} = 1.9\mathrm{pb}\ .$$

LHC: rate $\sim 10^5$ events/year with nominal luminosity ($10^{34}\,\mathrm{cm}^{-2}\mathrm{s}^{-1}$)

TCS at lower energies

Berger, Diehl, Pire, 2002

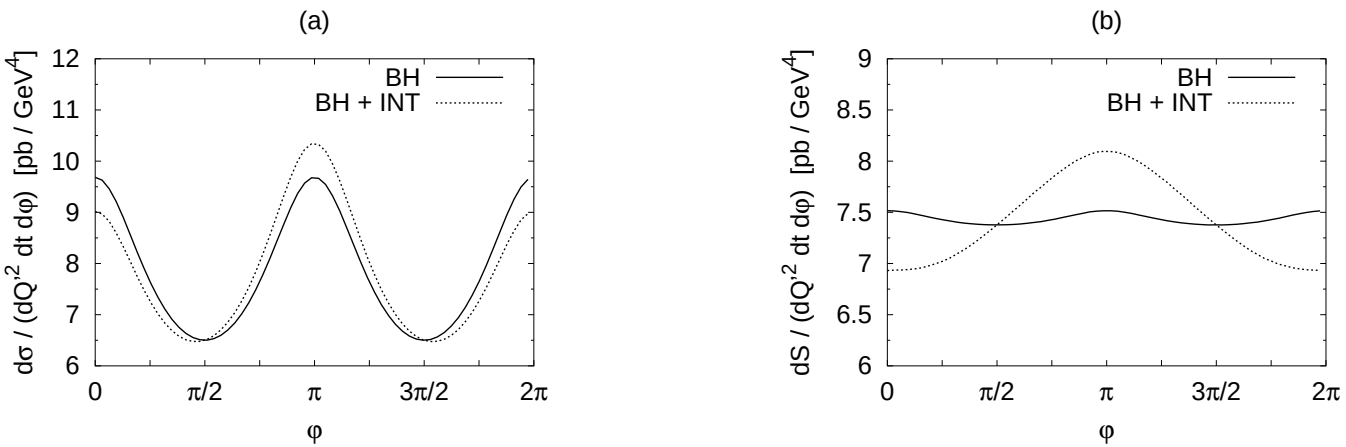

Figure:

B-H dominant; TCS dominated by quark GPDs

Charge asymmetry $\sim$ interference of B-H and TCS

TCS at lower energies

Problem with JLab data:

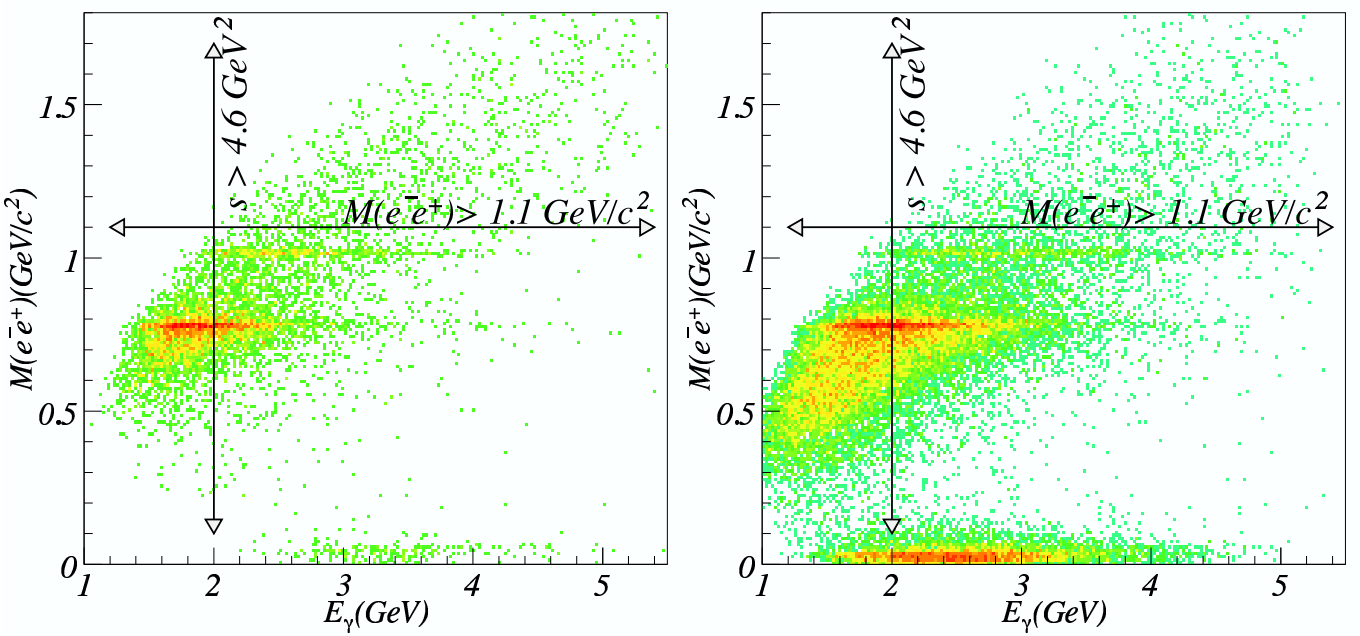

(a) (b)

Figure 4.7: e^-e^+ invariant mass distribution vs quasi-real photon energy. For TCS analysis $M(e^-e^+) > 1.1 GeV/c^2$ and $s > 4.6 GeV^2$ regions are chosen. Left graph represents e1-6 data set, right one is from e1f data set.

TCS at lower energies

NLO corrections necessary:

$$R = \frac{\int d\phi \ \cos(\phi) d\sigma}{\int d\phi \ d\sigma}$$

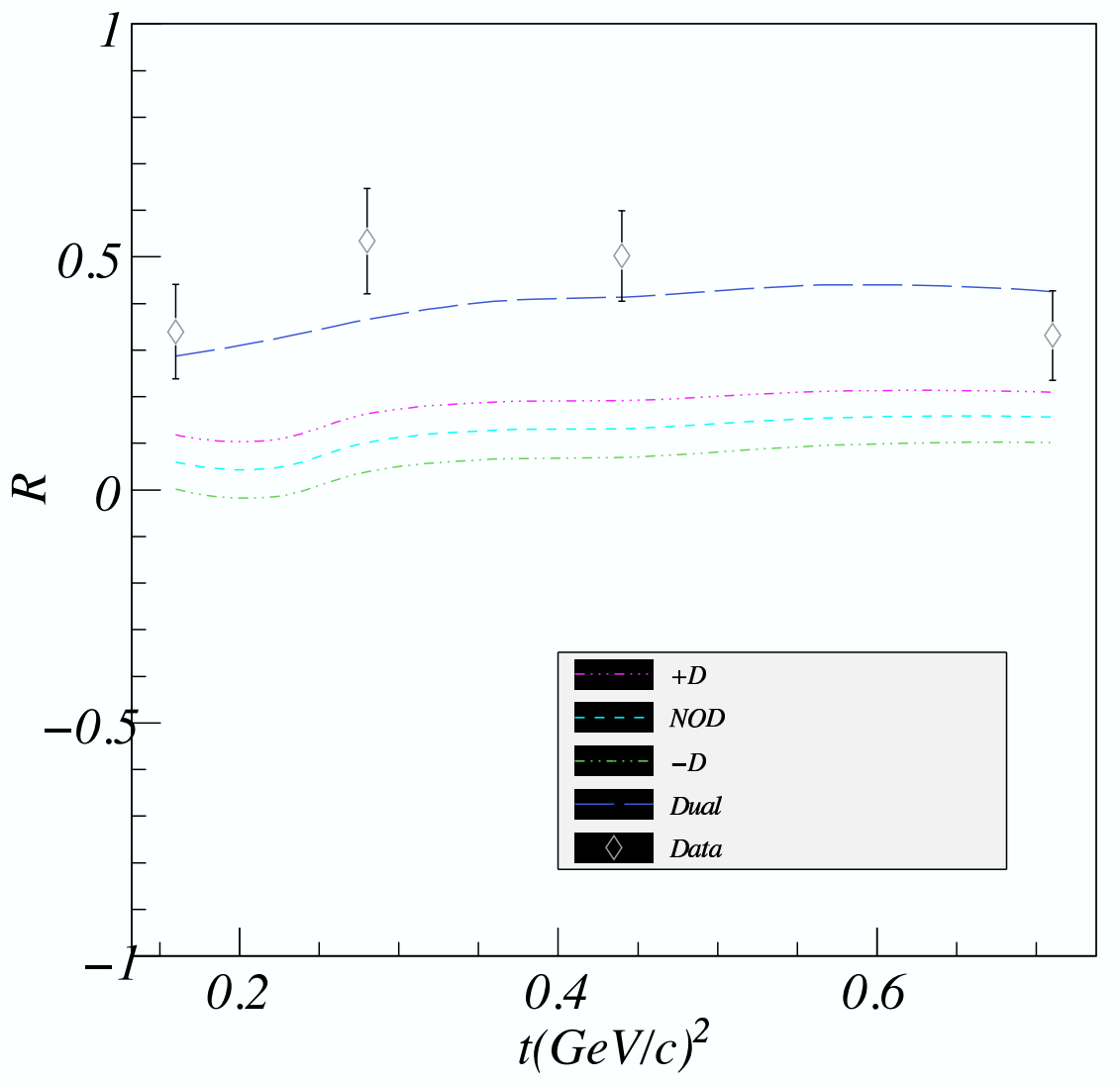

NLO corrections

$$\gamma^*(q_{in})N \to \gamma^*(q_{out})N'$$

DVCS versus TCS versus DDVCS:

- DVCS: $q_{in}^2 < 0\,, \quad q_{out}^2 = 0$
- TCS: $q_{in}^2 = 0\,, \quad q_{out}^2 > 0$
- DDVCS: $q_{in}^2 < 0\,, \quad q_{out}^2 > 0$

Why NLO corrections of TCS are interested:

- at high energies gluons important, they enter at NLO
- DIS versus Drell-Yan: big K-factors $\log \frac{-Q^2}{\mu_F^2} \to \log \frac{Q^2}{\mu_F^2} \pm i\pi$
- dependence (strong ?? or weak ??) on the factorization scale μ_F
- $\text{DVCS}_{unphysicalregion} \quad \xi \to \xi - i\varepsilon \quad \text{DVCS}_{physicalregion}$

in TCS and DDVCS it is not enough

Kinematics in Ji's (symmetric) notation

incoming photon $q_{in} = (q - \xi p)$ outgoing photon $(q_{out} = q + \xi p)$

incoming proton $P = (1 + \xi)p$ outgoing proton $P' = (1 - \xi)p$

$$\begin{aligned} p &= p^+(1,0,0,1)\,, \\ n &= \frac{1}{2p^+}(1,0,0,-1)\,, \\ q &= -x_B p + \frac{Q^2}{2x_B} n \end{aligned}$$

so: $pn = 1$, $s = (p+q)^2 = \frac{1-x_B}{x_B} Q^2$ and $x_B = \frac{Q^2}{s+Q^2}$

$$q_{in}^2 = -Q^2(1 + \frac{\xi}{x_B}) \quad q_{out}^2 = -Q^2(1 - \frac{\xi}{x_B})$$

DVCS: $x_B = \xi$, $Q^2 > 0$ TCS: $x_B = -\xi$, $Q^2 = -Q'^2 < 0$

DDVCS: $0 < x_B < \xi$ and $Q^2 > 0$ OR $0 > x_B > -\xi$ and $Q^2 < 0$

Amplitude:

$$\mathcal{A}^{\mu\nu} = g_T^{\mu\nu} \int_{-1}^{1} dx \left[\sum_q^{n_F} T^q(x) F^q(x) + T^g(x) F^g(x) \right]$$

where renormalized coefficient functions are given by:

$$\begin{aligned} T^q &= C_0^q + C_1^q + \frac{1}{2} \ln\left(\frac{|Q^2|}{\mu_F^2}\right) \cdot C_{coll}^q \,, \\ T^g &= C_1^g + \frac{1}{2} \ln\left(\frac{|Q^2|}{\mu_F^2}\right) \cdot C_{coll}^g \end{aligned}$$

and the GPDs are

$$\begin{aligned} F^q(x,\xi) &= \frac{1}{2} \int \frac{d\lambda}{2\pi} e^{-i\lambda x} \left\langle P' \middle| \bar{\psi}_q\left(\frac{\lambda}{2} n\right) \gamma^\mu \psi_q\left(-\frac{\lambda}{2} n\right) \middle| P \right\rangle n_\mu \,, \\ F^g(x,\xi) &= -\frac{1}{2x} \int \frac{d\lambda}{2\pi} e^{-i\lambda x} \left\langle P' \middle| F_a^{\mu\alpha}\left(\frac{\lambda}{2} n\right) F_{a\alpha}^{\nu}\left(-\frac{\lambda}{2} n\right) \middle| P \right\rangle n_\mu n_\nu \end{aligned}$$

Diagrams

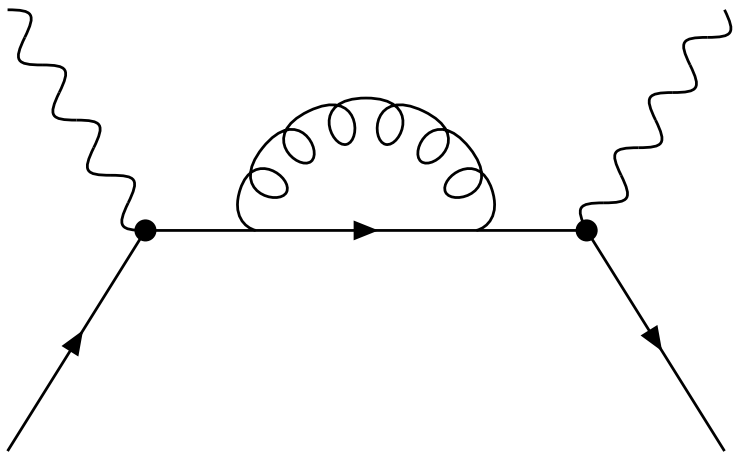

Figure: Self energy correction to $q\gamma \rightarrow q\gamma$ scattering amplitude

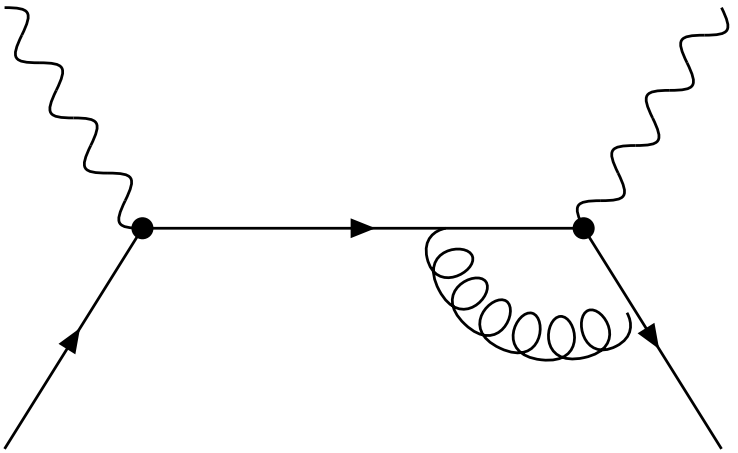

Figure: Right vertex correction to $q\gamma \to q\gamma$ scattering amplitude

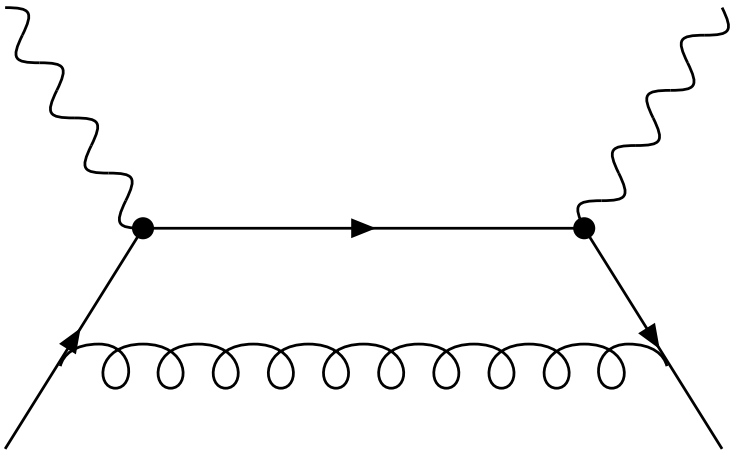

Figure: Box diagram correction to $q\gamma \to q\gamma$ scaterring amplitude

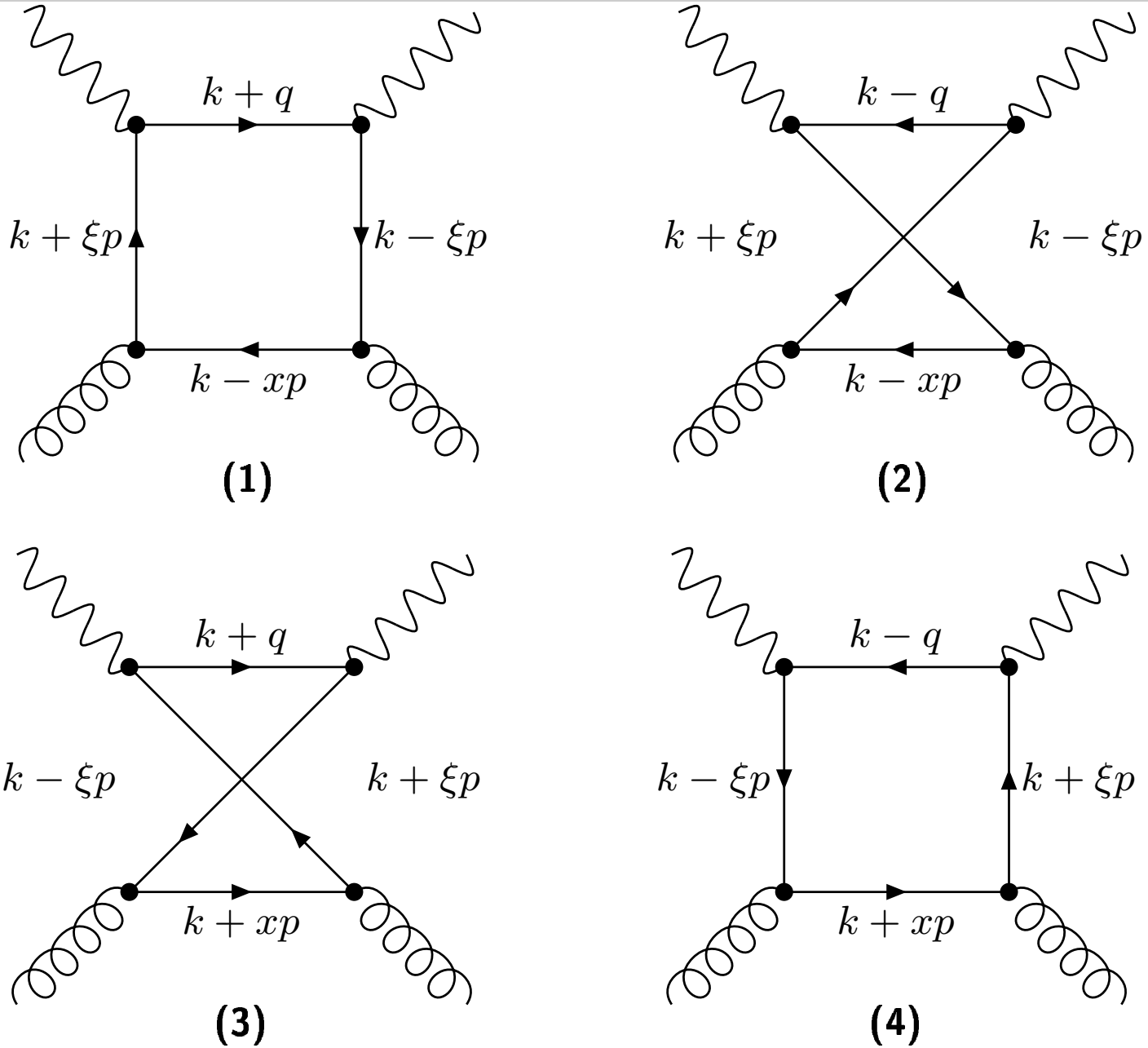

Figure: First group of diagrams describing $\gamma g \to \gamma g$ scattering.

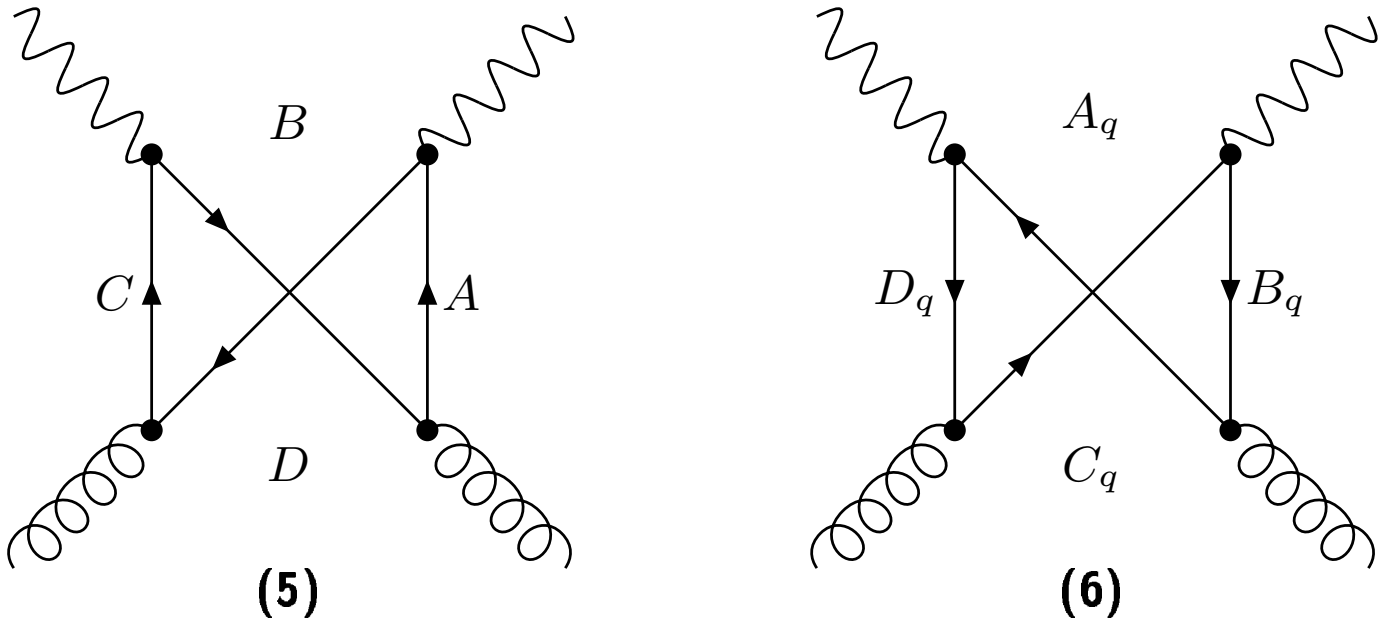

Figure: Second group of diagrams describing $\gamma g \to \gamma g$ scattering.

Results: TCS + DVCS + DDVCS

TCS:

Quark coefficient functions:

$$C_0^q = e_q^2 \left(\frac{1}{x-\xi-i\varepsilon} + \frac{1}{x+\xi+i\varepsilon} \right),$$

$$C_1^q = \frac{e_q^2 \alpha_S C_F}{4\pi}$$

$$\left\{ \frac{1}{x-\xi-i\varepsilon} \left[-9 + 3\log(-1+\frac{x}{\xi}-i\varepsilon) - 6\frac{\xi}{x+\xi}\log(-1+\frac{x}{\xi}-i\varepsilon) + 6\frac{\xi}{x+\xi}\log(-2-i\varepsilon) \right.\right.$$
$$\left. + \log^2(-1+\frac{x}{\xi}-i\varepsilon) - \log^2(-2-i\varepsilon) \right]$$
$$+ \frac{1}{x+\xi+i\varepsilon} \left[-9 + 3\log(-1-\frac{x}{\xi}-i\varepsilon) + 6\frac{\xi}{x-\xi}\log(-1-\frac{x}{\xi}-i\varepsilon) - 6\frac{\xi}{x-\xi}\log(-2-i\varepsilon) \right.$$
$$\left.\left. + \log^2(-1-\frac{x}{\xi}-i\varepsilon) - \log^2(-2-i\varepsilon) \right] \right\},$$

$$C_{coll}^q = \frac{e_q^2 \alpha_S C_F}{4\pi} \left\{ \frac{1}{x-\xi-i\varepsilon} \left[6 + 4\log(-1+\frac{x}{\xi}-i\varepsilon) - 4\log(-2-i\varepsilon) \right] \right.$$
$$\left. + \frac{1}{x+\xi+i\varepsilon} \left[6 + 4\log(-1-\frac{x}{\xi}-i\varepsilon) - 4\log(-2-i\varepsilon) \right] \right\}$$

Gluon coefficient functions:

$$C^g_{coll} = \frac{\left(\sum_q e_q^2\right)\alpha_S T_F}{4\pi}\frac{8x}{(x+\xi+i\varepsilon)(x-\xi-i\varepsilon)}\cdot$$

$$\left[\frac{x-\xi}{x+\xi}\log\left(-1+\frac{x}{\xi}-i\varepsilon\right)+\frac{x+\xi}{x-\xi}\log\left(-1-\frac{x}{\xi}-i\varepsilon\right)-2\frac{x^2+\xi^2}{x^2-\xi^2}\log(-2-i\varepsilon)\right],$$

$$C^g_1 = \frac{\left(\sum_q e_q^2\right)\alpha_S T_F}{4\pi}\frac{2x}{(x+\xi+i\varepsilon)(x-\xi-i\varepsilon)}\cdot$$

$$\begin{aligned}\Big[&-2\frac{x-3\xi}{x+\xi}\log\left(-1+\frac{x}{\xi}-i\varepsilon\right)+\frac{x-\xi}{x+\xi}\log^2\left(-1+\frac{x}{\xi}-i\varepsilon\right)\\&-2\frac{x+3\xi}{x-\xi}\log\left(-1-\frac{x}{\xi}-i\varepsilon\right)+\frac{x+\xi}{x-\xi}\log^2\left(-1-\frac{x}{\xi}-i\varepsilon\right)\\&+4\frac{x^2+3\xi^2}{x^2-\xi^2}\log(-2-i\varepsilon)-2\frac{x^2+\xi^2}{x^2-\xi^2}\log^2(-2-i\varepsilon)\Big]\end{aligned}$$

Discussion

- DVCS: the imaginary parts from $\xi \to \xi - i\varepsilon$
- TCS:
  - part of imaginary parts from $\xi \to \xi + i\varepsilon$
  - there appear e.g. $\log^2(-2 - i\varepsilon)$ which contribute to imaginary parts
  - in DVCS the imaginary part are in DGLAP region
    in TCS they are in DGLAP AND ERBL
- at LO: $C^q_{0(DVCS)} = {C^q_{0(TCS)}}^*$

  at NLO: $C^q_{coll(DVCS)} = {C^q_{coll(TCS)}}^*$ and $C^g_{coll(DVCS)} = {C^g_{coll(TCS)}}^*$

NLO quark:

$$\frac{C^{q}_{1(TCS)}{}^{*} - C^{q}_{1(DVCS)}}{\frac{e^2\alpha_S C_F}{4\pi}} =$$

$$\frac{1}{x-\xi+i\varepsilon}\left[\left(3-2\log 2+2\log|1-\frac{x}{\xi}|\right)(i\pi)+\pi^2\left(1+\theta(x-\xi)-\theta(-x+\xi)\right)\right]$$

$$+\frac{1}{x+\xi-i\varepsilon}\left[\left(3-2\log 2+2\log|1+\frac{x}{\xi}|\right)(i\pi)+\pi^2\left(1+\theta(-x-\xi)-\theta(x+\xi)\right)\right]$$

NLO gluon in DGLAP region:

$$\frac{C^{g}_{1(TCS)} - C^{g}_{1(DVCS)}}{\frac{\left(\sum_q e_q^2\right)\alpha_S T_F}{4\pi}} \overset{x\geq\xi}{=} \frac{2x}{x^2-\xi^2}\left[2\frac{x-\xi}{x+\xi}\pi^2\right.$$

$$\left.+\left(-4\frac{x-3\xi}{x+\xi}+2\frac{x-\xi}{x+\xi}\log|1-\frac{x}{\xi}|-2\frac{x+\xi}{x-\xi}\log|1+\frac{x}{\xi}|+4\frac{x^2+\xi^2}{x^2-\xi^2}\log 2\right)(-i\pi)\right]$$

quark ratio: $R^q = \dfrac{C_1^q + \frac{1}{2}\log\left(\frac{|Q^2|}{\mu_F^2}\right)\cdot C_{coll}^q}{C_0^q}$

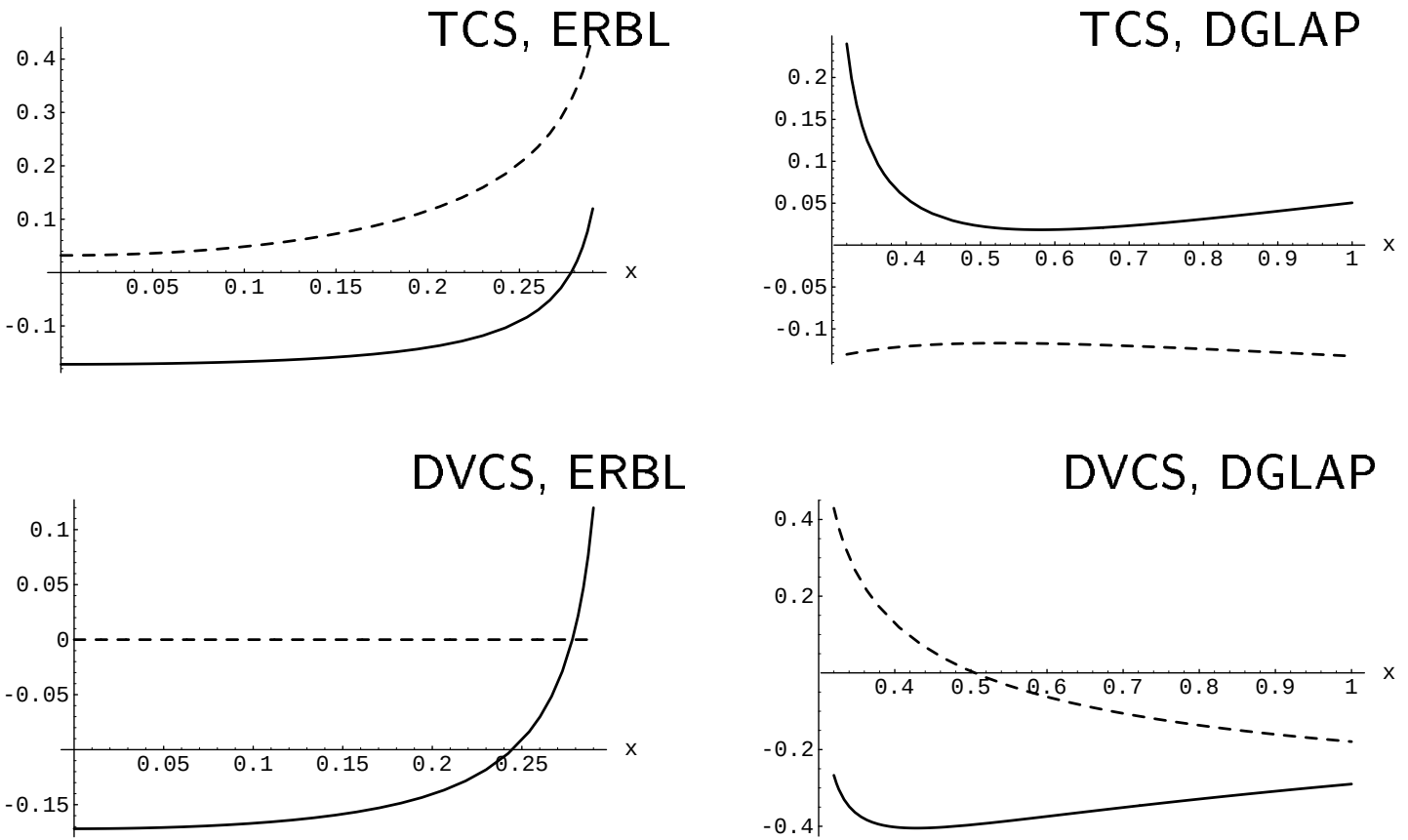

Figure: Real (solid line) and imaginary (dashed line) part of the ratio R^q of the NLO quark coefficient function to the Born term in Timelike Compton Scattering (up) and Deeply Virtual Compton Scattering (down) as a function of x in the ERBL (left) and DGLAP (right) region for $\xi = 0.3$, for $\mu_F^2 = |Q^2|$.

another quark ratio: $R^q_{T-S} = \dfrac{C^q_{1(TCS)} - C^{q\,*}_{1(DVCS)}}{C^q_0}$

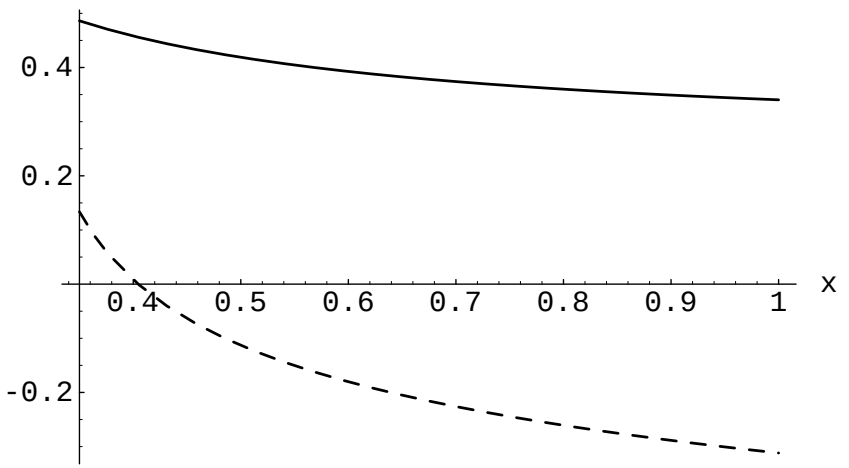

Figure: Real (solid line) and imaginary (dashed line) part of the ratio R^q_{T-S} of difference of NLO quark coefficient functions to the LO coefficient functions in the TCS and DVCS as a function of x in the DGLAP region for $\xi = 0.3$.

gluonic ratios:

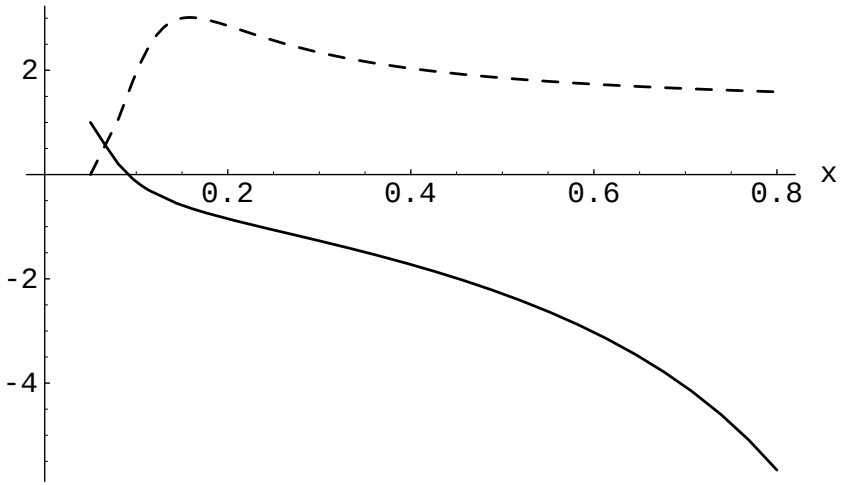

Figure: Ratio of the real (solid line) and imaginary (dashed line) part of the NLO gluon coefficient function in TCS to the same quantity in DVCS as a function of x in the DGLAP region for $\xi = 0.05$ for $\mu_F^2 = |Q^2|$.

Factorisation scale dependence of quark CF:

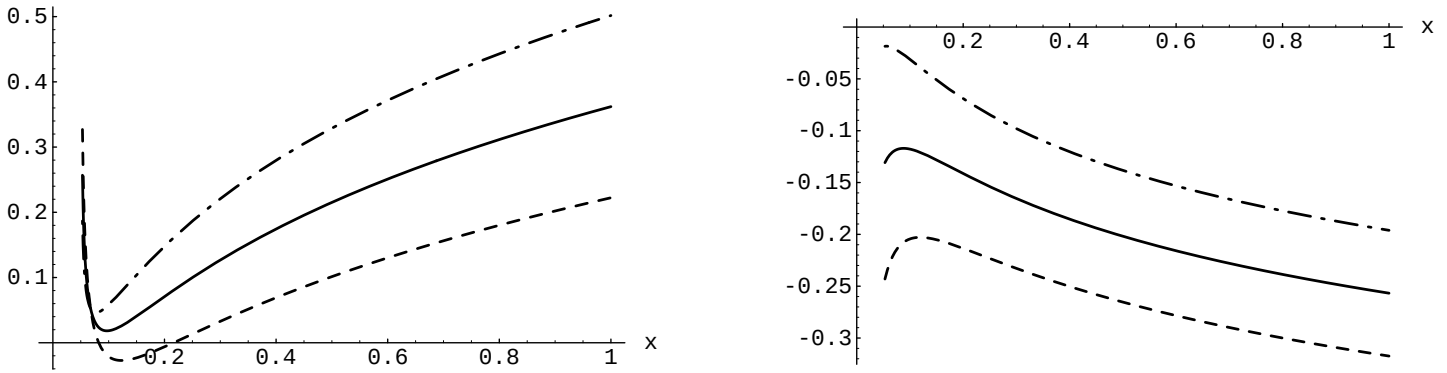

Figure: Factorization scale dependence of the real (left) and imaginary (right) parts of ratio R^q of NLO quark correction to hard scattering amplitudes to Born level coefficient function of the Timelike Compton Scattering as a function of x in the DGLAP region for $\xi = 0.05$. The ratios are plotted for the values of $\frac{|Q^2|}{\mu_F^2}$ equal 0.5 (dashed), 1 (solid) and 2 (dash-dotted line).

Factorisation scale dependence of gluonic CF:

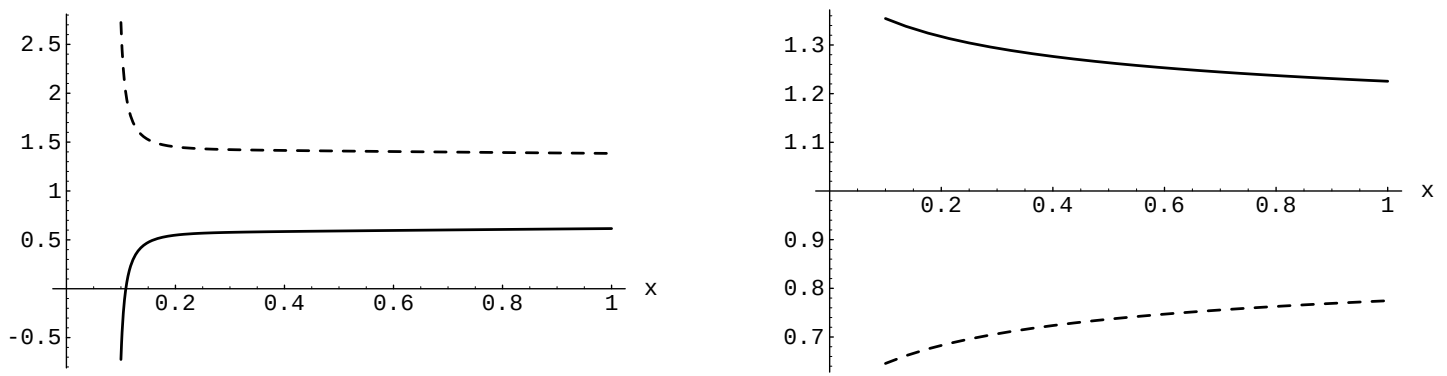

Figure: Ratios of the real (left) and imaginary (right) parts of NLO gluon coefficient function for $|Q^2| = 1/2\mu_F^2$ (solid line) and $|Q^2| = 2\mu_F^2$ (dashed line) to the same quantities with $|Q^2| = \mu_F^2$. Those quantities are calculated for the timelike Compton scattering and plotted as a function of x in the DGLAP region for $\xi = 0.05$.

Conclusions of the NLO part:

- new results: NLO corrections to TCS and to DDVCS
- corrections seem to be big ...
- better understanding of large terms (π^2, ??) is needed — resummation
- realistic phenomenology needed: — (in progress)
  - realistic GPD convoluted with our NLO CFs
  - calculation of relevant observables

Conclusions of the NLO part:

- new results: NLO corrections to TCS and to DDVCS
- corrections seem to be big ...
- better understanding of large terms (π^2, ??) is needed resummation ??
- realistic phenomenology needed: (in progress)
  - realistic GPD convoluted with our NLO CFs
  - calculation of relevant observables

- NICE DATA FROM JLAB, LHC, RHIC ON TCS, DDVCS ARE URGENTLY NEEDED !!